

Land and cryosphere products from Suomi NPP VIIRS: Overview and status

Christopher O. Justice,^{1,2} Miguel O. Román,^{2,3} Ivan Csiszar,⁴ Eric F. Vermote,³ Robert E. Wolfe,³ Simon J. Hook,⁵ Mark Friedl,⁶ Zhuosen Wang,^{7,8} Crystal B. Schaaf,^{7,8} Tomoaki Miura,⁹ Mark Tschudi,¹⁰ George Riggs,^{11,12} Dorothy K. Hall,¹² Alexei I. Lyapustin,¹³ Sadashiva Devadiga,^{3,14} Carol Davidson,^{3,14} and Edward J. Masuoka³

Received 18 June 2013; revised 15 August 2013; accepted 15 August 2013; published 11 September 2013.

[1] The Visible Infrared Imaging Radiometer Suite (VIIRS) instrument was launched in October 2011 as part of the Suomi National Polar-Orbiting Partnership (S-NPP). The VIIRS instrument was designed to improve upon the capabilities of the operational Advanced Very High Resolution Radiometer and provide observation continuity with NASA's Earth Observing System's Moderate Resolution Imaging Spectroradiometer (MODIS). Since the VIIRS first-light images were received in November 2011, NASA- and NOAA-funded scientists have been working to evaluate the instrument performance and generate land and cryosphere products to meet the needs of the NOAA operational users and the NASA science community. NOAA's focus has been on refining a suite of operational products known as Environmental Data Records (EDRs), which were developed according to project specifications under the National Polar-Orbiting Environmental Satellite System. The NASA S-NPP Science Team has focused on evaluating the EDRs for science use, developing and testing additional products to meet science data needs, and providing MODIS data product continuity. This paper presents to-date findings of the NASA Science Team's evaluation of the VIIRS land and cryosphere EDRs, specifically Surface Reflectance, Land Surface Temperature, Surface Albedo, Vegetation Indices, Surface Type, Active Fires, Snow Cover, Ice Surface Temperature, and Sea Ice Characterization. The study concludes that, for MODIS data product continuity and earth system science, an enhanced suite of land and cryosphere products and associated data system capabilities are needed beyond the EDRs currently available from the VIIRS.

Citation: Justice, C. O., et al. (2013), Land and cryosphere products from Suomi NPP VIIRS: Overview and status, *J. Geophys. Res. Atmos.*, 118, 9753–9765, doi:10.1002/jgrd.50771.

1. The S-NPP Mission and the VIIRS Instrument for Land Remote Sensing

[2] The Visible Infrared Imaging Radiometer Suite (VIIRS) instrument was launched in October 2011 as part of the

NPOESS (National Polar-orbiting Environmental Satellite System) Preparatory Project (NPP), subsequently renamed the Suomi National Polar-orbiting Partnership (S-NPP) in January 2012. S-NPP was planned as a bridging mission intended to provide observation continuity with NASA's

The copyright line for this article was changed on 22 August 2014.

¹Department of Geographical Sciences, University of Maryland, College Park, Maryland, USA.

²These authors contributed equally to this work.

³Terrestrial Information Systems Laboratory, NASA Goddard Space Flight Center, Greenbelt, Maryland, USA.

⁴NOAA Center for Satellite Applications and Research, College Park, Maryland, USA.

Corresponding author: C. O. Justice, Department of Geographical Sciences, University of Maryland, College Park, MD 20782, USA. (justice@umes.geog.umd.edu)

M. O. Román, Terrestrial Information Systems Laboratory, NASA Goddard Space Flight Center, Greenbelt, MD 20771, USA. (miguel.o.roman@nasa.gov)

©2014 The Authors.

This is an open access article under the terms of the Creative Commons Attribution-NonCommercial-NoDerivs License, which permits use and distribution in any medium, provided the original work is properly cited, the use is non-commercial and no modifications or adaptations are made.

2169-897X/13/10.1002/jgrd.50771

⁵Jet Propulsion Laboratory, California Institute of Technology, Pasadena, California, USA.

⁶Department of Earth and Environment, Boston University, Boston, Massachusetts, USA.

⁷Department of Environmental, Earth and Ocean Sciences, University of Massachusetts, Boston, Massachusetts, USA.

⁸Center for Remote Sensing Department of Earth and Environment, Boston University, Boston, Massachusetts, USA.

⁹Department of Natural Resources and Environmental Management, University of Hawaii at Manoa, Honolulu, Hawaii, USA.

¹⁰Colorado Center for Astrodynamics Research, University of Colorado, Boulder, Colorado, USA.

¹¹Science Systems & Applications, Inc., NASA Goddard Space Flight Center, Lanham, Maryland, USA.

¹²Cryospheric Sciences Laboratory, NASA Goddard Space Flight Center, Greenbelt, Maryland, USA.

¹³Climate and Radiation Laboratory, NASA Goddard Space Flight Center, Greenbelt, Maryland, USA.

¹⁴Sigma Space Corporation, NASA Goddard Space Flight Center, Greenbelt, Maryland, USA.

Earth Observing System (EOS) and the operational VIIRS instruments to be flown on the first Joint Polar-Orbiting Satellite System (JPSS-1) in 2017. The VIIRS instrument is intended to improve upon the operational Advanced Very High Resolution Radiometer (AVHRR) and provide continuity with the EOS Moderate Resolution Imaging Spectroradiometer (MODIS). Since the VIIRS first-light images were received in November 2011, NASA and NOAA scientists have been working to evaluate the instrument on-orbit performance and generate land and cryosphere products to meet the needs of the NOAA operational user community and NASA science. NOAA's focus has been on refining and validating a suite of operational products known as Environmental Data Records (EDRs), developed by Northrop Grumman and Raytheon according to project specifications. The NASA NPP Science Team has focused on evaluating the EDRs for science use and developing and testing additional or improved VIIRS products to meet outstanding science data needs and provide MODIS data continuity. The S-NPP has had a dynamic and complex history with roles and responsibilities changing between federal agencies and private contractors. With the emphasis of the program on meeting operational user needs, the bulk of the resources and effort to generate land and cryosphere products from S-NPP have been focused on the contractor-developed EDRs [Justice et al., 2011].

[3] The primary target audience for the NOAA EDRs is the traditional NOAA operational users, such as the National Weather Service and the Air Force Weather Agency. Data from the VIIRS are being used to generate land and cryosphere EDRs (hereby termed EDRs or "VIIRS products") for use in a number of operational applications, ranging from real-time weather operations to forecast model input and environmental monitoring applications. The VIIRS products are currently being processed in NOAA's near-real-time Interface Data Processing Segment (IDPS), which receives raw instrument data and telemetry from the ground stations supporting the S-NPP mission. The IDPS converts the Raw Data Records, generated by sensors on S-NPP, into calibrated geolocated measurements called Sensor Data Records (SDRs) and then into geophysical parameters or Environmental Data Records (EDRs). In addition to SDRs and EDRs, the IDPS produces Intermediate Products (IPs) and Application-Related Products (ARPs). Application-Related Products (ARPs) are a subcategory of EDRs and are subject to the same latency requirements. Intermediate Products (IPs) are produced as an interim step in the EDR processing and (for the S-NPP mission) are stored for long-term archiving. These products are archived and distributed by NOAA's Comprehensive Large Array-Data Stewardship System (CLASS).

[4] The standard VIIRS IDPS-generated products (EDRs, ARPs, and IPs) are only produced in swath-based Level 2 format. Thus, only information from a single orbit is used, and available "per-pixel" information from overlapping swaths is not used. In contrast, the MODIS land products are stored using the Level 2 Grid (L2G) approach, which provides users with the original observations and their subpixel geolocation information. The rationale behind the L2G approach was to select the observations least affected by off-nadir viewing observations while maximizing coverage within a cell of the gridded projection. This improves the efficiency of processing and reprocessing of L2G and higher-level gridded products.

[5] Early versions of the VIIRS Land EDRs have been available since "first light" to allow data users to gain familiarity

with data formats and parameters. In the first 12 months of on-orbit operations, three major baseline releases (termed IDPS Mx5.3, Mx6.2, and Mx6.3) were installed to deliver product fixes and look-up table updates. However, the products have undergone limited "Beta" testing and in some cases contain significant errors. Further detailed evaluation is needed to determine their suitability for quantitative scientific studies [Román et al., 2012]. As the VIIRS on-orbit performance has stabilized and ground-truth campaigns and data examination exercises are generating results, the NOAA JPSS Land Product Algorithm Development and Cal/Val team and the NASA S-NPP VIIRS Land discipline team are working toward bringing EDRs to "provisional" status by the end of 2013.

2. VIIRS Land EDR Evaluation and Status

[6] As with the MODIS products, the VIIRS Land EDRs can be grouped into four general product categories: (1) radiation budget variables, i.e., the Surface Reflectance (corrected for effects of the atmosphere), Land Surface Temperature (LST), and Surface Albedo; (2) ecosystem variables, i.e., Vegetation Indices (VI); (3) land-cover characteristics, i.e., Surface Type (ST) and the location of Active Fires; and (4) cryospheric products, i.e., Snow Cover, Ice Surface Temperature (IST) and Sea Ice Characterization (SIC). A number of these products, including the Surface Reflectance, have their heritage in the MODIS product algorithms, and in some cases early versions of the MODIS code were used by the contractor in the VIIRS product algorithm development. The Land Group of NASA's S-NPP Science Team is evaluating the suitability of the VIIRS Land algorithms in terms of their ability to fulfill NASA's science needs. It should be noted that data from the VIIRS Land Product Evaluation and Analysis Tool Element's (Land PEATE) archive sets (AS) 3001 (products generated by the Land PEATE using the IDPS software) and AS 3002 (products generated by the Land PEATE using NASA Land Science Team adjusted versions of the IDPS software) were used in the evaluation of the VIIRS EDRs (cf. section 3 for a description of the Land PEATE). The improvements performed as part of AS 3002 included algorithm improvements, bug fixes, and look-up table updates. In most cases, these adjustments were implemented months before they transitioned into operational production in the IDPS (AS 3001).

2.1. Land Surface Temperature

[7] The VIIRS Land Surface Temperature (LST) EDR provides the skin temperature of the uppermost layer of the land surface (and larger inland waters) in swath format, equivalent to the MODIS Level 2 product. The EDR deviates from its MODIS counterpart in a few ways: (1) it has a functional dependency on previously generated surface type dependent coefficients; (2) it does not provide dynamic land emissivity per the current MODIS day-night product, MOD11B1 [Wan and Li, 1997], or MODIS temperature emissivity separation product, MOD21 [Hulley et al., 2010]; and (3) the fall-back two-band split-window algorithm (employed when cloud cover or strong atmospheric effects are detected) uses both thermal and middle-infrared bands. Surface emissivity is known to change under many circumstances, including rainfall in arid regions, phenological changes, and intrasurface type changes or fires. This variation is not fully

Table 1. JPSS Accuracy Requirements (Threshold and Objective as Listed in Version 2.7 of the JPSS Level 1 Requirements Supplement) and Estimated Performance Based on NASA VIIRS Science Team Evaluations To-Date^a

EDR, IP, or ARP	Threshold	Objective	Estimate (Evaluation Scenario)
Land Surface Temperature ^b	1.4 K	0.8 K	~ 1.0 K (dense vegetation and water) > 2.5 K (semiarid, seasonally varying landscapes)
Surface Reflectance ^c	$\pm (0.01 + 10\%)$	$\pm (0.005 + 5\%)$	≤ 0.015 (dense vegetation and dark surfaces) > 0.015 (bright surfaces)
Surface Albedo	0.08	0.0125	> 0.078 (CEOS LPV sites and desert sites)
Vegetation Index (TOA NDVI)	0.05	0.03	< 0.030 (nadir view over Western Hemisphere versus MODIS Aqua)
Vegetation Index (TOC EVI)	0.05	N/S	< 0.030 ^d (nadir view over Western Hemisphere versus MODIS Aqua)
Active Fires ^e	[1.0, 5,000 MW]	[1.0, 10,000 MW]	N/S
Surface Type ^f	70% PCT	80% PCT	~ 70% PCT (IGBP Classes 0–5, 10, 12–13, 15–16) < 70% PCT (IGBP Classes 6–9, 11, 14)
Snow Cover ^g	90% PCT	90% PCT	~ 90% PCT (midlatitude and high-latitude regions)
Ice Age	70% PCT ^h	90% PCT ^h	> 70% PCT ⁱ (polar regions, all seasons) < 70% PCT ^h (polar regions, all seasons)
Ice Concentration	N/S ^j	N/S	Good agreement versus MODIS sea ice extent (polar regions, all seasons)
Ice Surface Temperature	1.0 Kelvin ^k	N/S	< 0.2 K (versus MODIS IST) < 0.5 K (versus KT-19 observations, Ice Bridge cal/val campaign)

^aNote that additional specifications typically apply to each product, such as revisit time, coverage, long-term stability and mapping, precision, and uncertainty; for brevity, these are not listed here. Further, each product has an associated set of exclusion conditions (e.g., high solar zenith angles) for which its specifications are relaxed. N/S = No value specified. PCT = Probability of correct typing.

^bResults are based on IDPS MX6.2 build, after a look-up table update was implemented.

^cNote that performance is dependent on both the spectral band and magnitude of the reflectance (e.g., increased surface brightness results in a multiplicative error of 5%).

^dWith EVI gain adjusted to 2.5.

^eFire Radiative Power (FRP) measurement range threshold requirement. The high end of the FRP measurement range threshold requirement (5000 MW) is based on current design capabilities (i.e., the present 634 K saturation specification for the VIIRS M13 Band) and the recommendation of the NOAA-NASA Land Science Team. Quantitative assessment of ARP product is pending on availability of quality reference data, primarily from airborne measurements.

^fSeventeen-class IGBP classification.

^gApplies only to snow/no-snow classification.

^hIce-free, new/young ice, all other ice.

ⁱIce/ice-free classification.

^jVIIRS produces a sea ice concentration IP in clear sky conditions, which is provided as an input to the Ice Surface Temperature calculation.

^kUncertainty requirement for Ice Surface Temperature.

captured in the current IDPS version of the VIIRS product. Previous work has shown that for arid and semiarid regions, a better approach is to use an algorithm with dynamically varying emissivity, such as is used in the MOD11B1 or MOD21 products [Hulley and Hook, 2009]. For continuity, the generation of an emissivity product compatible with MODIS is desired, i.e., a merged product using both split-window and dynamic emissivity retrieval.

[8] The measurement accuracy (bias) and precision (1 sigma) specified for the VIIRS LST product are 1.4 and 0.5 K, respectively, which must be met when the VIIRS Cloud Mask indicates a high confidence of clear conditions (cf. Table 1). The dynamic range for the product extends from 213 to 343 K. The product is being generated over all land pixels except when conditions mentioned above are not met, as determined from the VIIRS Cloud Mask (VCM).

[9] Initial evaluation of the VIIRS Land Surface Temperature (LST) EDR (based on IDPS Mx6.2) was performed using three different approaches: (1) cross comparison with the Aqua MODIS LST product (MOD11) when the Aqua and S-NPP overpasses were within 30 min of each other; (2) absolute temperature validation using the Lake Tahoe and Salton Sea automated validation approach [Hook et al., 2007]; and (3) radiance-based (R-based) LST validation over a set of pseudo-invariant sites [Wan and Li, 2008]. The R-based method provides estimates of the true LST using a radiative closure

simulation without the need for in situ measurements and requires input air temperature, relative humidity profiles, and emissivity data [Hulley and Hook, 2012].

[10] Figure 1 shows a plot of the validation results using MOD11, MOD21, and VIIRS for the Kelso Dunes pseudo-invariant field site using data from AS 3001 and AS 3002. Note that, at the time of this exercise, the baseline algorithm available at the IDPS (AS 3001) was the “fallback” split-window (land-cover-based approach) retrieval method. In contrast, the baseline algorithm available at the Land PEATE was the two-band, split-window algorithm.

[11] This case highlights the problem of using a static map for the emissivity coefficients seen with both the MOD11 and VIIRS products [Hulley and Hook, 2009]. In both cases the retrieved MOD11 and VIIRS LSTs are too low by 2–3 K (emissivity set too high), whereas the dynamic emissivity approach MOD21 gives the better answer. As a result, the VIIRS LST EDR retrieval does not meet the accuracy threshold requirement. In summary, while the VIIRS Land Surface Temperature EDR is shown to be good to 1 K over dense vegetation and water, users should beware of major deficiencies in the current IDPS algorithm, particularly over semiarid and seasonally varying regions, where large errors of several degrees kelvin have been found. Long-term validation is needed as well as additional comparisons with data from other instruments.

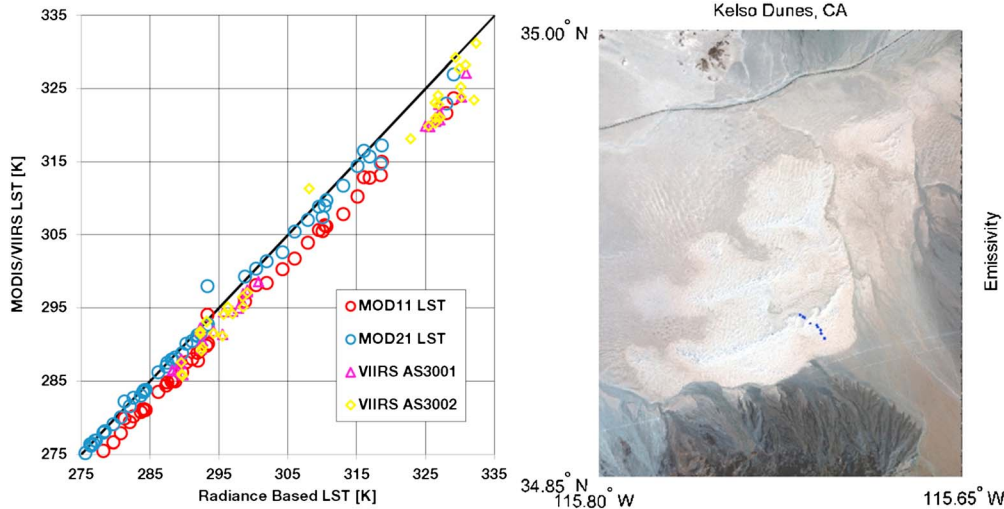


Figure 1. (left) Plot of MODIS/VIIRS LST at the Kelso Dunes, California, pseudo-invariant site (image on right) versus radiance-based LST.

2.2. Surface Reflectance

[12] Surface reflectance is one of the key products from VIIRS and, as with MODIS, is used in developing several higher-order land and cryosphere products, including Global Climate Modeling Grid (CMG) products (cf. Figure 2), which are used as input for modeling global trends. The VIIRS Surface Reflectance IP is based on the heritage MODIS Collection 5 product [Vermote *et al.*, 2002], which provides atmospherically corrected reflectances for the VIIRS bands M1, M2, M3, M4, M5, M7, M8, M10, and M11 for each moderate resolution pixel and for the VIIRS bands I1, I2, and I3 for each imagery resolution pixel. The quality and character of surface reflectance depend largely on the accuracy of the VCM and aerosol algorithms.

[13] A preliminary assessment of the VCM shows that the product correctly detects large, bright, and cold clouds and significantly underestimates small and low cumulus clouds. In part, this is a consequence of VCM being designed to satisfy all EDR algorithms and thus provide an average performance in terms of omission and commission errors, in contrast to the

more conservative MODIS cloud mask. The leakage of small clouds creates large biases in the VIIRS Surface Reflectance IP, which are not currently captured by the quality flags.

[14] The quality of VIIRS aerosol retrievals is still being evaluated by the VIIRS Land and Aerosol cal/val teams, and a detailed picture has yet to emerge. At present, the VIIRS aerosol algorithm does not provide aerosol type (model) information, and its aerosol optical depth (AOD) product is of lower quality, often significantly, than that of MODIS. The deficiencies are most apparent over bright surfaces, where VIIRS often shows high AOD values when in fact it is clear. Over moderately bright and dark surfaces, VIIRS AOD rather unpredictably may show a substantial bias, which could stem from the adopted flexible selection of the aerosol model on a pixel basis [H. Liu *et al.*, Validation of Suomi-NPP VIIRS Aerosol Optical Thickness, submitted to *Journal of Geophysical Research: Atmospheres*, 2013].

[15] The VIIRS SDR, and particularly the associated calibration, is being closely monitored on a continuous basis by cross comparison of the VIIRS and MODIS Surface Reflectance product over instrumented field sites. At this early stage, we

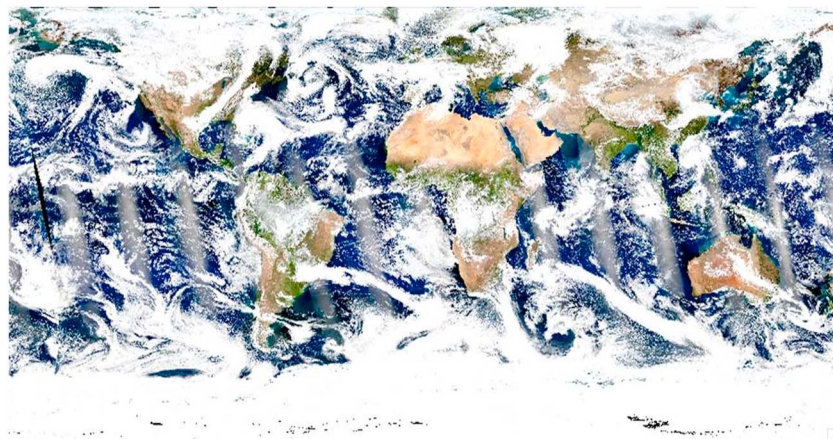


Figure 2. VIIRS Level 3 Global 0.05 Degree Global Climate Modeling Grid (CMG) Surface Reflectance Intermediate Product (Land PEATE-adjusted version of the Surface Reflectance IP IDPS algorithm) for 26 October 2012.

Table 2. Average Surface Reflectance and Bias of VIIRS Surface Reflectance IP for Selected Sites^a

Site Name	M2 (436–454 nm)		M4 (545–565 nm)		M5 (662–682 nm)		M7 (846–885 nm)	
	Reflectance	Bias	Reflectance	Bias	Reflectance	Bias	Reflectance	Bias
Sites that have a relatively good performance with biases								
UCSB	0.042	-0.007	0.070	-0.006	0.084	-0.005	0.230	-0.005
Cuiaba-Miranda	0.033	0.004	0.069	0.000	0.084	-0.002	0.254	-0.006
Ispra	0.029	-0.013	0.055	-0.009	0.045	-0.006	0.297	-0.006
Evora	0.058	-0.004	0.106	-0.005	0.157	-0.007	0.300	-0.009
Konza	0.039	-0.004	0.077	-0.006	0.084	-0.007	0.302	-0.014
Alta Floresta	0.036	-0.003	0.078	-0.005	0.094	-0.003	0.321	-0.008
Bondville	0.027	-0.010	0.059	-0.004	0.052	-0.005	0.348	0.012
Lille	0.042	-0.015	0.081	-0.011	0.074	-0.009	0.355	-0.001
Sites that have a marginal performance								
Table Mountain	0.082	-0.017	0.123	-0.014	0.156	-0.011	0.250	-0.008
Railroad Valley	0.123	-0.018	0.183	-0.015	0.229	-0.014	0.273	-0.010
Goddard Space Flight Center	0.038	-0.026	0.063	-0.018	0.053	-0.019	0.295	-0.008
Hamburg	0.032	-0.012	0.071	-0.011	0.060	-0.010	0.345	-0.007
Sites of poor performance								
Beijing	0.058	-0.032	0.086	-0.022	0.086	-0.022	0.255	-0.009
XiangHe	0.039	-0.019	0.072	-0.017	0.062	-0.011	0.326	-0.007
Dakar	0.079	-0.028	0.132	-0.037	0.147	-0.028	0.328	-0.086
Banizoumbou	0.066	0.021	0.174	-0.005	0.298	-0.029	0.467	-0.049

^aThe analysis covered the period of January–October 2012 based on $50 \times 50 \text{ km}^2$ subsets of VIIRS data gridded to 0.750 km resolution over the AERONET sites. The full analysis includes Accuracy or bias, Precision, and Total Uncertainty (APU) for different levels of surface brightness in each target area. Results here provide a cumulative evaluation for the average reflectance level.

can confirm that the VIIRS SDR is suitable for generating Surface Reflectance IP; however, continuous monitoring is necessary, and in the absence of any reprocessing, data generated prior to the VIIRS SDR provisional status (March 2013) might not be suitable for the Surface Reflectance IP.

[16] An evaluation of the VIIRS Surface Reflectance IP was performed based on accuracy assessments over several Aerosol Robotic Network (AERONET)-based Surface Reflectance Validation Network sites [Wang *et al.*, 2009]. Results are summarized in Table 2. The data are organized to indicate an average performance level over regions with relatively low cloudiness, good AERONET record (without gaps in the measurements), and high retrieval statistics. The top part of Table 2 indicates sites that have a relatively good performance with biases across all spectral bands below 0.015. These study sites are characterized by an abundance of vegetation and

relatively dark surfaces, with the exception of the University of California, Santa Barbara (UCSB) site. The middle part of Table 2 indicates sites that have a marginal performance, and the bottom part of Table 2 indicates sites of poor performance. Of these, the high biases for the Beijing and XiangHe are due to the high aerosol levels, and Dakar and Banizoumbou have bright surfaces where the VIIRS aerosol retrievals are problematic.

2.3. Surface Albedo

[17] Albedo, the quantity that specifies the proportion of the shortwave radiative flux that is reflected by the surface, is one of the primary VIIRS Land EDRs as well as being one of the Global Climate Observing System's Essential Climate Variables [Schaaf *et al.*, 2011]. The VIIRS EDR specification calls for only a broadband (0.3–4.0 μm) value, retrieved on a

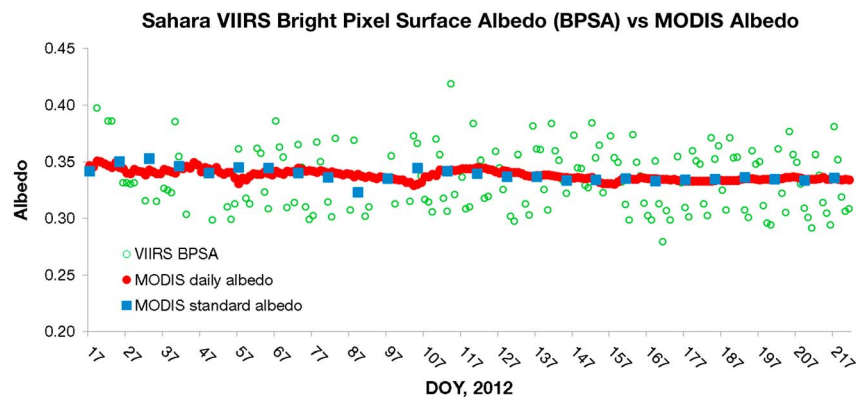


Figure 3. Comparison between VIIRS Bright Pixel Surface Albedo (BPSA) (green circles), MODIS Collection 5 eight-day standard product (blue squares), and MODIS Collection 6 daily albedo (analogous to the VIIRS Dark Pixel Surface Albedo (DPSA), red circles) over the Sahara site (a stable desert location: 26.450°N, 14.083°E) for 17 January to 4 August 2012. Daily BPSA varies between 0.29 and 0.40 in the Sahara. A recent look-up table (LUT) reduces this somewhat, but view-angle effects still dominate (LUT implemented 18 January 2013). A solution suggested to reduce variability is to simply implement a multiday average.

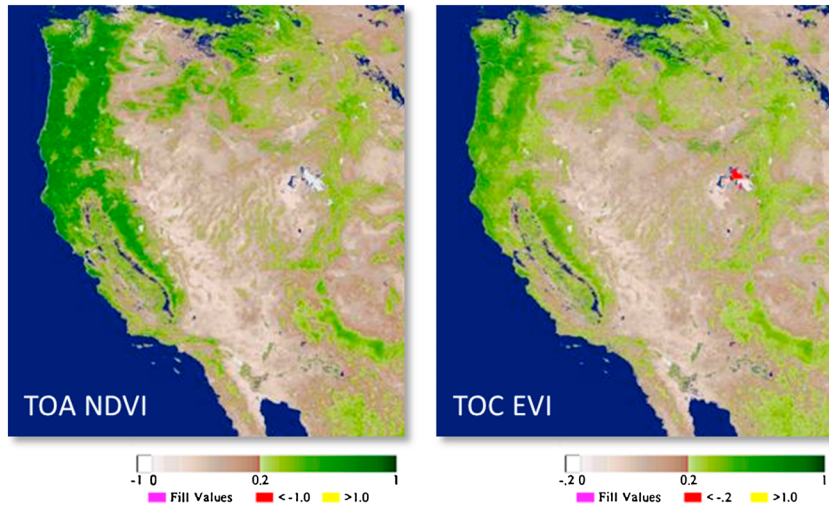


Figure 4. VIIRS Vegetation Index EDR, top-of-atmosphere (TOA) NDVI (left) and top-of-canopy (TOC) EVI (right) for 1 October 2012 (day of year 163-IDPS Mx6.3.)

daily basis under cloud-free conditions. Two algorithms have been implemented as part of the Albedo EDR to fulfill this operational requirement. The first (designated as a Dark Pixel Surface Albedo or DPSA) is derived from the validated MODIS heritage [Cescatti *et al.*, 2012; Román *et al.*, 2009; Schaaf *et al.*, 2002] and relies on the periodic multiday retrieval of narrowband anisotropy models to estimate the Bidirectional Reflectance Distribution Function (BRDF) of each field of view [Lucht *et al.*, 2000; Wanner *et al.*, 1995]. These periodic models are then coupled with the surface reflectance retrieved on any single day to obtain an estimate of the daily shortwave albedo at the overpass time. Similar approaches have been employed with data from Multi-angle Imaging SpectroRadiometer (MISR), Meteosat, Meteosat Second Generation (MSG)/Seviri, and MEedium Resolution Imaging Spectrometer (MERIS) GLOBAlbedo. The second approach (designated as a Bright Pixel Surface Albedo or BPSA) relies on top-of-atmosphere radiance measurements at overpass time and precomputed radiative transfer model information to estimate daily broadband surface albedos [Liang, 2003].

[18] Only the BPSA output has been produced since launch. After concern over the VIIRS Rotating Telescope Assembly degradation subsided [Barrie *et al.*, 2012], daily records of the BPSA product were investigated over several field sites. Results were noisy and variable, a condition ascribed to poor cloud clearing or atmospheric correction. However, investigation of IDPS BPSA outputs (version Mx6.2) over a location in the Sahara (26.450°N , 14.083°E) revealed that this variability continued over what should have been a stable calibration location (cf. Figure 3). A look-up table correction over the summer of 2012 exacerbated the problem. Investigation of recent studies using the BPSA approach indicate that averaging (both spatially and temporally) can be used to derive a stable product [He *et al.*, 2012]. On the other hand, when daily estimates from the VIIRS were tested using the MODIS daily algorithm code [Wang *et al.*, 2012], the results were stable and similar to what is achieved with MODIS data. While efforts to incorporate surface BRDF in the construction of linear regression models to estimate broadband albedo are being examined [Wang *et al.*, submitted to *Journal of Geophysical Research: Atmospheres*, 2013], the operational BPSA algorithm has yet

to undergo substantial code changes, unit testing, and evaluation exercises, making it at this time unusable for land studies. Therefore, while the VIIRS input spectral data is behaving well, users should beware of the deficiencies inherent in the current baseline algorithm (the BPSA) and should refrain from using the Albedo EDR in science applications until such problems are addressed.

2.4. Vegetation Index

[19] The VIIRS Vegetation Index (VI) EDR currently consists of two products generated daily at the imagery resolution (0.375 km at nadir) over land in swath form (Figure 4): the Normalized-Difference Vegetation Index (NDVI) from top-of-atmosphere (TOA) reflectances (ρ_{TOA}) [Tucker, 1979] and the Enhanced Vegetation Index (EVI) from atmospherically corrected, top-of-canopy (TOC) reflectance (ρ_{TOC}):

$$\text{NDVI} = (\rho_{\text{TOA}}^{\text{TOA}} - \rho_{\text{TOA}}^{\text{TOA}}) / (\rho_{\text{TOA}}^{\text{TOA}} + \rho_{\text{TOA}}^{\text{TOA}}) \quad (1)$$

$$\text{EVI} = (1 + L) \cdot \frac{\rho_{\text{TOC}}^{\text{TOC}} - \rho_{\text{TOC}}^{\text{TOC}}}{\rho_{\text{TOC}}^{\text{TOC}} + C_{11} \cdot \rho_{\text{TOC}}^{\text{TOC}} - C_{M3} \cdot \rho_{M3}^{\text{TOC}} + L} \quad (2)$$

where the spectral bands I1 and I2 are the VIIRS channels in the 600–680 nm and 845.5–884.5 nm bands, respectively; L , C_{11} , and C_{M3} are constants; and $M3$ is the spectral band from 478–498 nm. The $M3$ band (0.750 km at nadir) has twice the cell dimension of the I1 and I2 bands (0.375 km at nadir), and its value is applied to four equivalent-area array cells. The VIIRS VI EDR has adopted the earlier form of the EVI equation from the MODIS Vegetation Index Algorithm Theoretical Basis Document [Huete *et al.*, 1999, equation 12, p. 33]. In VIIRS EVI, the gain factor to set the dynamic range ($1 + L$) is linked to the canopy background brightness adjustment factor (L), whereas the gain factor (G) can be set independent of the canopy background brightness factor (L) in the actual MODIS EVI equation. In the current VIIRS algorithm, L is set to 1.0, and so the gain factor becomes 2. In the MODIS EVI equation, the gain factor G is set to 2.5 ($G = 2.5$). Note that, while the MODIS and VIIRS EVI products are produced with different gain factors, their basic functionality should be equivalent [Vargas *et al.*, submitted to *Journal of Geophysical Research: Atmospheres*, 2013].

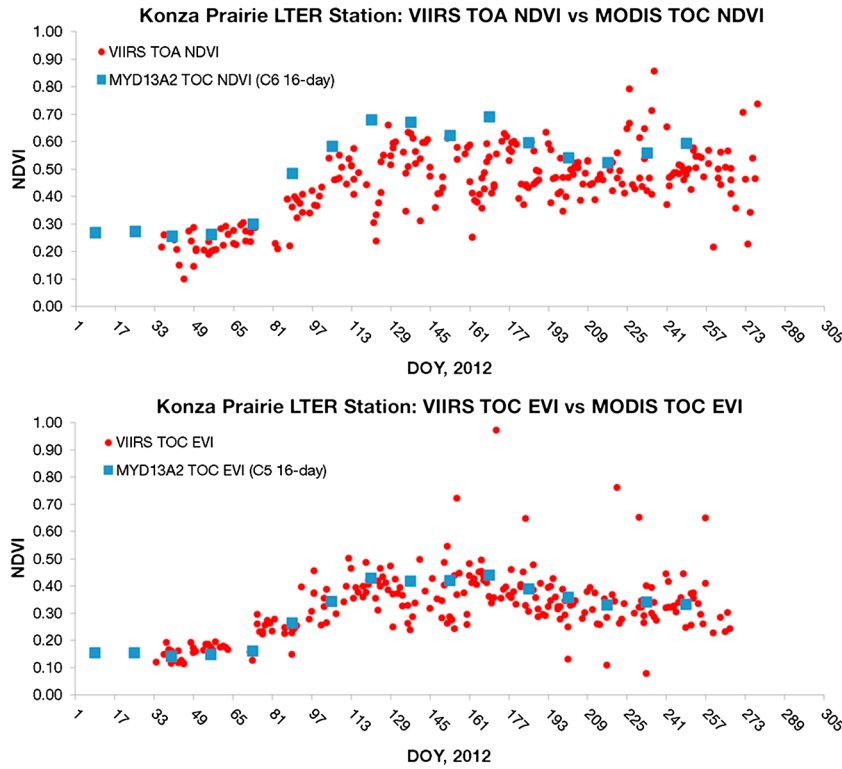


Figure 5. VIIRS Vegetation Index EDR (red circles) temporal profiles (3 km-by-3 km window) over the Konza Prairie Long-Term Ecological Research (LTER) station depicting seasonal changes comparable to those of Aqua MODIS (blue squares).

[20] The VI EDR is based on bidirectional reflectance factor estimates, representing intrinsic measurements for actual sensor view and sun angle conditions [Schaepman-Strub *et al.*, 2006]. The EDR includes quality flags on land/water, cloud confidence, including thin cirrus, heavy aerosol loadings, and exclusion conditions.

[21] In general, the VIIRS VI EDR is radiometrically performing well. Both TOA NDVI and TOC EVI depict spatial variations of global vegetation cover well without any noticeable sensor noise. The VIIRS TOA NDVI and TOC EVI retrievals compare consistently well with those derived from Aqua MODIS for good observations obtained along their overlapped ground tracks (*i.e.*, near-nadir, cloud, cloud shadow, snow/ice-free, and clear atmosphere). Their differences (VIIRS versus MODIS) show consistent patterns since February 2012. Temporal profiles of VIIRS TOA NDVI and TOC EVI show seasonal evolutions that correspond to vegetation growth over a wide variety of land-cover conditions, which are comparable to those depicted in the Aqua MODIS VI time series (cf. Figure 5).

[22] In detail, the current EDR contains several types of erroneous observations and retrievals. First, both the TOA NDVI and TOC EVI are subject to cloud contamination. Recurrent instances of cloudy pixels have been found that were undetected by the upstream processing (*i.e.*, by the VCM) or that could not properly be screened with the current set of VI quality flags (QFs). Second, the current VI EDR also contains observations that are of low or suspicious quality. These include cloud shadow, adjacency cloud, snow/ice cover, and fire, all of which are not flagged by the current IDPS algorithm or the current set of quality flags. Without a major

revamp of the existing VI quality assurance fields, as well as compositing to reduce this contamination to a standard view and solar geometry, the VIIRS VI temporal profiles (and thus, any long-term data records derived from this product) will continue to show secondary variations that can be larger than the seasonal changes, particularly over forested areas.

[23] For the VIIRS TOC EVI retrieval, spatial gaps in the data have been found; particularly due to unavailability of M3 TOC reflectance. These conditions frequently occur over bright pixels (desert areas), and are likely a result of overcorrection of the atmosphere associated with overestimated VIIRS Aerosol Optical Thickness. The TOC EVI product often contains unrealistically high or small values over snow/ice cover and also over cloud-contaminated pixels. Finally, due to the different gain factor from the heritage MODIS sensor, the dynamic range of the VIIRS EVI is ~20% less than that of the MODIS EVI. An algorithm change request to use the MODIS EVI equation is currently under consideration. Looking forward, the inclusion of a TOC NDVI, which is missing from the current product suite, has also been included in the revised Level 1 requirements for the JPSS program.

2.5. Ice Temperature and Characterization

[24] The VIIRS Ice Surface Temperature (IST) EDR provides a skin temperature for sea-ice covered areas. In this context, sea ice is considered to be ice and any overlying snow, given that bare ice exists for only a short period during the summer or when new ice is forming. The IST EDR (Figure 6, left) is produced for clear skies both day and night over the oceans. It does not include areas of freshwater ice. For these areas, surface temperatures are provided by the

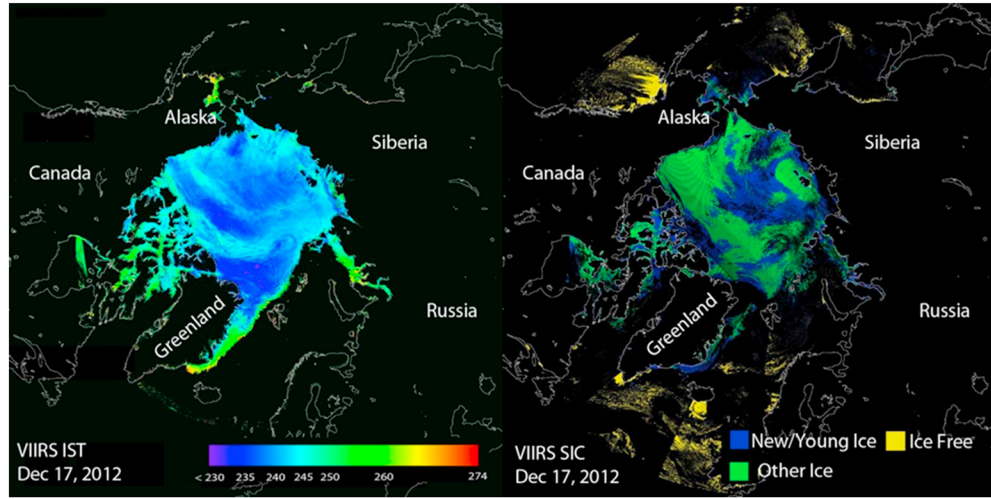


Figure 6. Composites of VIIRS Ice Surface Temperature (IST) EDR (left) and VIIRS Sea Ice Characterization (SIC) EDR (right) for 17 December 2012 over the Arctic.

LST EDR. The VIIRS IST algorithm employs the same type of statistical linear multichannel regression approach as the LST EDR. It uses a split-window approach, regressing the VIIRS M11 and M12 bands against observed temperatures, thus depending on available IST observations.

[25] Validation of the VIIRS IST EDR has been done primarily through comparisons to the MODIS IST product (similar algorithm) and KT-19 measurements from the NASA IceBridge aircraft. Results from an IceBridge comparison show good agreement, with the VIIRS IST less than 0.5 K warmer than the KT-19 observations and less than 0.2 K warmer than the MODIS IST [Key et al., submitted to *Journal of Geophysical Research: Atmospheres*, 2013]. Updating the regression coefficients with more robust training data may reduce biases. However, this process is limited by the availability of good observations for algorithm tuning and the accuracies of the supporting IPs. Given that IST retrievals are only done for clear sky conditions, there is a strong dependence on the VCM. Validation of both the IST and the Sea Ice Characterization EDRs indicates that errors in the VCM

at high latitudes are common and problematic. Potential improvement in the VCM for polar regions is therefore essential for improving the IST EDR.

[26] The VIIRS Sea Ice Characterization (SIC) EDR (Figure 6, right) uses the SIC IP as a primary input. There is no heritage MODIS product for the SIC EDR (MODIS is ice extent only). The product consists of an ice age classification map that contains classifications for "Ice-free," "New/Young Ice," and "All Other Ice" categories. New/Young Ice has a maximum thickness of 30 cm, while All Other Ice is thicker than 30 cm. The EDR does not include freshwater ice and may also exclude some shore-fast ice areas, depending on the land mask used. It is produced both day and night over the oceans. The requirement for this EDR is 70% probability of correct ice typing. The VIIRS SIC algorithm uses inputs such as cloud properties, near surface wind speed, vapor pressure, surface temperature, albedo, and snow depth, which are used to solve the energy budget for ice thickness. The algorithm has a daytime (reflectance threshold) branch and a nighttime (energy balance) branch. The nighttime algorithm does

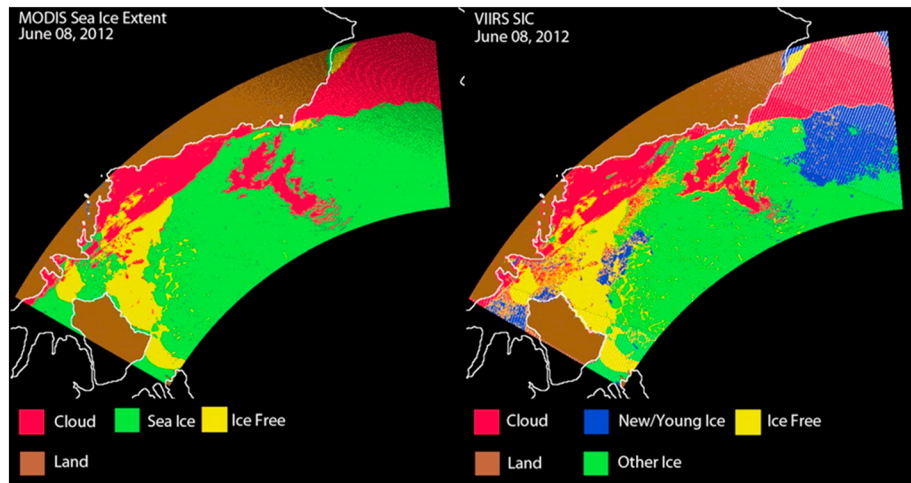


Figure 7. MODIS sea ice extent (left) and VIIRS Sea Ice Characterization (SIC) (right) for 8 June 2012 over the Beaufort Sea.

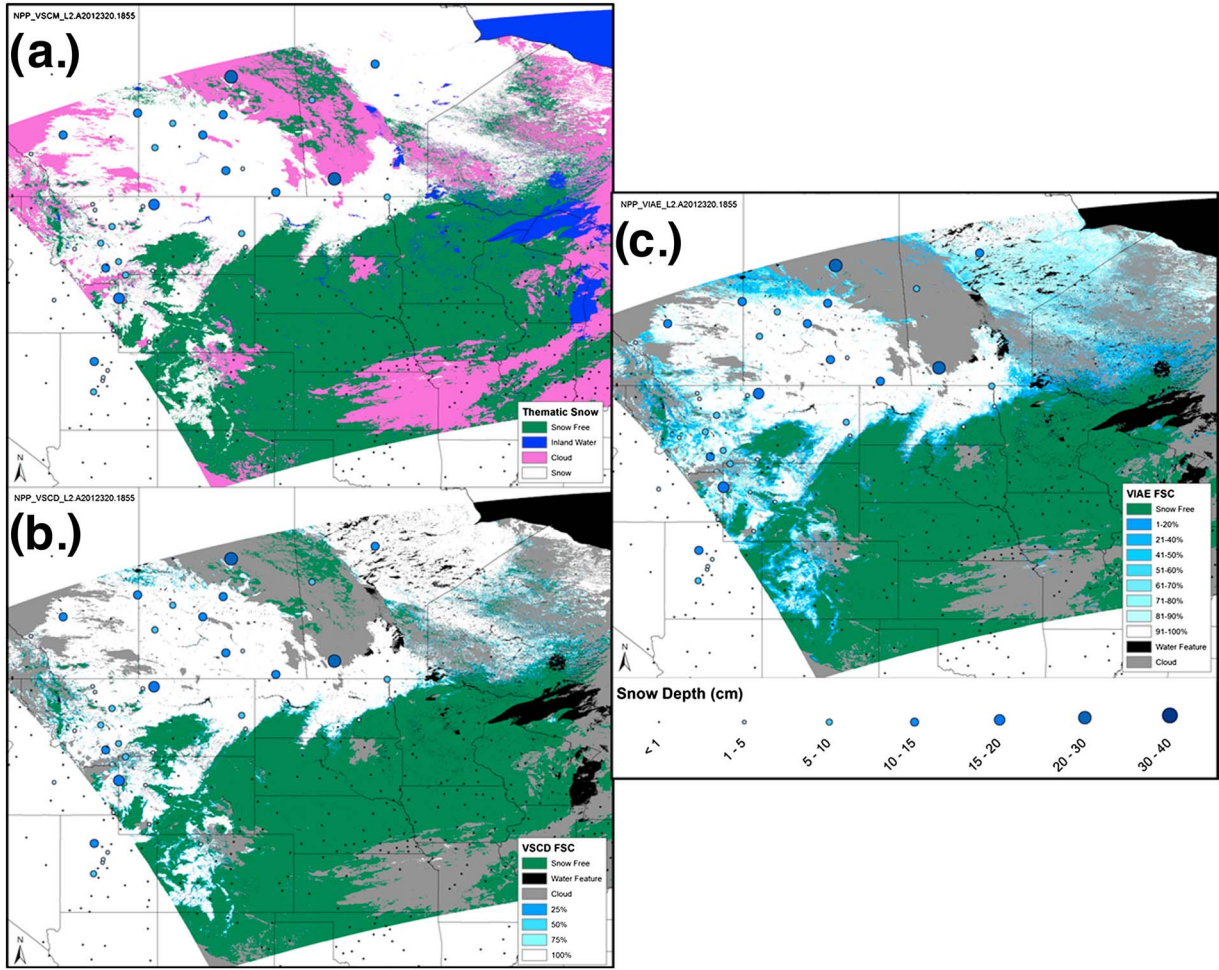


Figure 8. (a) VIIRS Snow Cover Binary Map (NPP_VSCM) compared to (b) Level 2 VIIRS Snow Fraction Product at 750 m (NPP_VSCD) and (c) VIIRS fractional snow cover based on MODIS heritage algorithm using the Level 1 VIIRS Sensor Data Record (SDR) at 375 m (NPP_VIAE). (NPP_VIAE) (acquired 15 November 2012).

not utilize albedo as input, relying more on the IST EDR to determine ice growth and subsequent thickness.

[27] The SIC EDR in its present form is unlikely to meet the specification of 70% probability for correct classification. Although the SIC IP agrees well with the MODIS sea ice extent product for comparisons performed in the Beaufort Sea region, the classification of ice type by the SIC EDR varies in accuracy. The SIC EDR is thus likely to be useful for identification of ice versus ice-free areas, but currently, there is no specification for this capability. The SIC EDR algorithm exhibits reasonable classification in some cases, although improvements to the algorithm will need to be devised and tested to overcome significant classification errors. Some misclassification appears to be caused by errors in snow depth parameterization, which is currently based on climatology. False ice is often observed near cloud edges. For the SIC EDR daytime branch of the algorithm during the melt season, misclassifications occur when the lower reflectance of melting sea ice appears to cause the SIC EDR to indicate New/Young Ice, although this type of ice cannot be present this time of year (cf. Figure 7, right). Note, however, that the distribution of ice and ice-free areas compares well with the MODIS sea ice extent in this example. For the nighttime branch of the SIC

EDR, ice misclassifications have been found that are likely due to low opacity clouds or ice fog, which result in errors to the IST IP that are in turn passed to the SIC EDR [Key *et al.*, submitted to *Journal of Geophysical Research: Atmospheres*, 2013].

2.6. Snow Cover

[28] The VIIRS Snow Cover suite of products includes the VIIRS Snow Cover Binary EDR and the VIIRS Snow Cover Fraction EDR. The Snow Cover Binary EDR is a swath product, produced at 0.375 km maximum spatial resolution in the daytime. Snow is identified only for pixels defined as “confidently clear” by the VCM. The requirement for this EDR is 90% probability of correct typing. The algorithm heritage is the MODIS snow cover algorithm, a normalized-difference snow index (NDSI) based algorithm that screens for snow detection errors [Salomonson and Appel, 2004]. The VIIRS Snow Cover Binary EDR is limited to an NDSI range of [0.4–1.0] for snow detection. Quality flags (QF) are set for input data quality, cloud information, and scene conditions and are extracted for quality assessment and to make thematic maps of snow cover extent (i.e., to include clouds and water bodies).

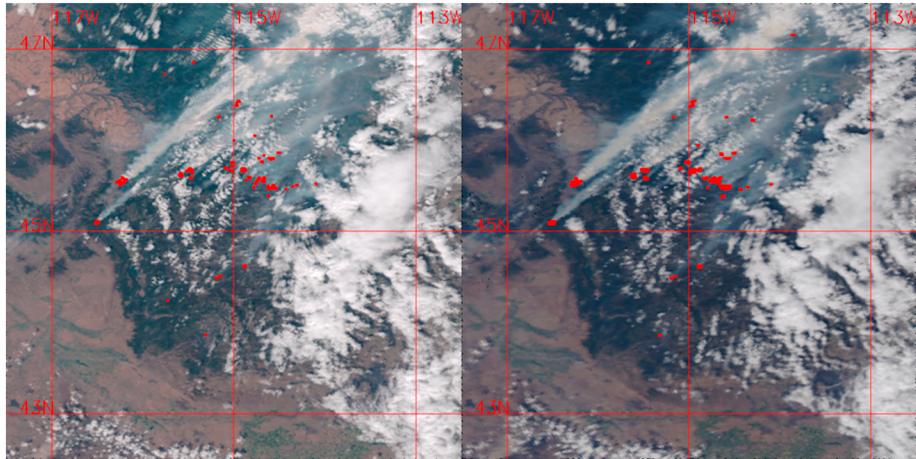


Figure 9. Comparison of Suomi NPP VIIRS (left) and Aqua MODIS (right) fire detections on 9 September 2012 at 19:55 and 20:15 UTC, respectively. The images show the Wesley, Sheep, McGuire, Porcupine, Mustang, Halstead, and Trinity Ridge fires in the Western U.S.

[29] The VIIRS Snow Cover Fraction EDR is generated by spatially aggregating four (i.e., 2×2) adjacent pixels in the Binary Snow Cover EDR to generate the fractional snow cover values using five discrete classes at 0.750 km resolution: 0, 25, 50, 75, and 100%. Quality flags from the VIIRS Snow Cover Binary EDR are aggregated in the Snow Fraction algorithm's QF data. There is no similarity between the VIIRS Snow Cover Fraction EDR and the MODIS Level-2 fractional snow cover algorithm. The latter is based on a NDSI regression using reflectance for input to estimate fractional snow cover continuously over the 1–100% range [Salomonson and Appel, 2004]. The VIIRS Snow Cover Fraction EDR maps the same snow extent as the VIIRS Binary Snow Cover EDR but at a coarser resolution.

[30] A preliminary evaluation of the VIIRS Snow Cover EDR shows that it is similar in accuracy to its MODIS counterpart (MYD10) in mapping snow cover extent [Key et al., submitted to *Journal of Geophysical Research: Atmospheres*, 2013]. Confusion between clouds and snow that decreases accuracy in snow extent exists in both products. Note that the Snow Cover Binary EDR uses the same NDSI algorithm as MODIS to map snow cover but uses a different wavelength (VIIRS 0.640 μm versus MODIS 0.555 μm). The difference in visible bands may have an effect on sensitivity or threshold selection of the NDSI for snow cover mapping, but this effect has yet to be investigated. Since the VIIRS Snow Cover Binary EDR and MODIS are similar, the working assumption is that the VIIRS product has an overall accuracy of ~90%, similar to that of MODIS in clear conditions. The VIIRS Snow Cover Binary EDR accuracy and quality has been observed to be static over seasons and many situations compared to the MYD10 and other snow cover maps. Snow/cloud or cloud/snow confusion causes snow commission or omission errors. These vary spatially and temporally in a scene and across seasons, with a typical range of 0–10% of pixels in a scene, depending on cloud and illumination conditions in the scene.

[31] In its current form, the VIIRS Snow Cover Fraction EDR is less accurate than the VIIRS Snow Cover Binary EDR. A revised version of the VIIRS Snow Cover Fraction EDR was developed by adapting the MODIS Collection 6 fractional

snow algorithm to the VIIRS data and is being run in the Land PEATE (Figure 8c). Retrievals of fractional cover are based on the full range of NDSI (0.0–1.0) at the VIIRS imagery resolution (0.375 km). These improvements are shown to reduce omission and commission errors and improve retrieval accuracy for mapping snow cover extent—a critical factor in predicting snowmelt runoff.

2.7. Active Fires

[32] The VIIRS Active Fires Application-Related Product (ARP) was built on the EOS MODIS Collection 4 Fire and Thermal Anomalies algorithm [Justice et al., 2002]. The main tests designed to identify fire-affected pixels in the image swath data mimic the MODIS algorithm with no specific tuning or consideration of unique spectral and/or spatial characteristics involving the primary VIIRS fire channels used (i.e., the 3.9–4.1 μm [M13] and 10.2–11.2 μm [M15] bands). In comparing VIIRS with MODIS Aqua (similar overpass times) the primary driver of differences in the products is related to spatial sampling. There are differences in pixel size, along scan line aggregation schemes, and line spread function. Future algorithm improvement plans include implementation of VIIRS-specific detection algorithm modifications, a Fire Radiative Power product, and a prototype I-band (375 m) fire detection product. These will be followed by implementing an Active Fire Climate Modeling Grid (CMG—0.05°) product.

[33] Assessment of the VIIRS Active Fires ARP has focused on qualitative comparisons with near-coincident Aqua/MODIS using the fire detection flag (i.e., fire/no-fire). Quantitative assessment of the Fire Radiative Power (FRP) output, which is included in the experimental algorithm toward a product compatible with MODIS [Csiszar et al., submitted to *Journal of Geophysical Research: Atmospheres*, 2013], is pending on availability of quality reference data, primarily from airborne measurements. Assessment of the VIIRS Active Fires ARP during the first year of data shows excellent instrument performance (Figure 9). Results also show consistency with Aqua/MODIS detections across variable viewing conditions, as well as good agreement over fire perimeters from the US Forest Service [cf. Csiszar et al., submitted to *Journal of Geophysical Research: Atmospheres*, 2013,

Figures 5–8]. In terms of algorithm performance, the current product shows satisfactory results with good overall correlation with near-coincident Aqua/MODIS active fire product data. However, false alarms leading to large clusters of spurious fire pixels occasionally occur due to inappropriate handling of the input SDR quality flags. This and earlier quality issues have been documented [Csiszar *et al.*, 2012]. Improvements to the VIIRS Active Fire ARP are being developed and run in the Land PEATE. There is no burned area product currently being generated from VIIRS.

2.8. Surface Type

[34] The VIIRS Surface Type EDR is a swath product built by reprojecting the VIIRS Gridded Quarterly Surface Type IP and overlaying it with the Active Fire ARP, Snow Cover EDR, and Vegetation Fractional Greenness products. It is produced at 1.0 km spatial resolution based on the previous 12 months of VIIRS data. The EDR provides 17 surface type classes following the International Geosphere-Biosphere Programme (IGBP) classification scheme [Belward *et al.*, 1999; Friedl *et al.*, 2002]. The requirement for this EDR is a 70% metric of correct classification. Off-the-shelf commercial software is used to generate the Gridded Quarterly Surface Type IP, which provides the foundation for the EDR. The algorithm uses an ensemble decision tree classifier to perform a supervised classification of global VIIRS data using a set of global training sites [Quinlan, 1996]. Input features include spectral information and temporal metrics developed from 12 months of VIIRS visible and infrared band information. Note that, because the Gridded Quarterly Surface Type IP requires a full year of input data from VIIRS, evaluation of the IP and EDR currently relies on prototype results from MODIS.

[35] The Surface Type EDR is expected to meet its target requirement of 70% overall classification accuracy. However, uniform land-cover types (e.g., barren/sparsely vegetated; permanent snow, and ice) are likely to have much higher classification accuracies than more complex and less separable classes. Results using MODIS data demonstrate that the algorithm is working but also indicate significant challenges related to confusion among specific classes that are also problematic in the MODIS Collection 5 land-cover product (e.g., shrublands, savannas, and mixture classes, such as the agricultural mosaic) [Friedl *et al.*, 2010]. The agriculture class, because of its global extent and diversity, is also challenging to map. It is unlikely that these issues will be resolved when the Quarterly Surface Type IP and Surface Type EDR are generated from VIIRS data. Thus, the VIIRS Surface Type EDR's accuracy will be below the 70% target for some classes. Differences in classification results across time will introduce spurious land-cover changes that are also difficult to address in the current algorithm implementation.

3. Data Generation and Distribution of VIIRS Land and Cryosphere Products

[36] For the S-NPP mission, NOAA's CLASS provides the main archive for the IDPS-generated products and is the primary facility for long-term archiving of these products. Note, however, that the primary focus of CLASS is data preservation and not on distribution (e.g., postprocessing is currently limited to band subsetting and aggregation, and common services such as spatial subsetting and reprojection are not available).

In addition to NOAA CLASS, the VIIRS Land PEATE, which is collocated with the MODIS Land production facilities, has a number of capabilities to support land science users of VIIRS data and leverages NASA's experience in the production of global land measurements [Masuoka *et al.*, 2011]. These include support for evaluation against MODIS science products, quality assessment and validation, and a test bed for algorithm changes [Román *et al.*, 2011; Wolfe *et al.*, 2010]. In a number of cases, the NASA VIIRS land and cryosphere teams are developing and testing MODIS continuity or improved algorithms at the Land PEATE, as described above.

[37] Currently, the Land PEATE aggregates the IDPS products into standard 5 min "MODIS-like" granules and distributes the data through NASA's Level 1 and Atmosphere Archive and Distribution System (LAADS) [Masuoka *et al.*, 2007] in a compact HDF4 format that is compatible with standard EOS MODIS products. The Land PEATE also produces daily and multiday global gridded (Level 3) versions of the IDPS EDR products that can be compared to the similar MODIS products. These data are made available to the NASA VIIRS Land Science Team and the broader community through the LAADS.

[38] To aid in understanding of the VIIRS instrument's capabilities for NASA earth science research and develop the long-term data record, the Land PEATE is working to regenerate the SDR and Land EDR, ARP, and IP products from January 2012 to the present, using the best available calibration and latest available algorithm changes. A number of algorithm changes recommended by the science team as a result of this evaluation will be included, and L3 daily and multiday gridded products will be generated. The results of this exercise will enable the science team to more fully evaluate the VIIRS instrument's usefulness in producing high-quality science data products and demonstrate improvements that could be made to the NOAA products. This reprocessing will also fulfill a requirement to provide reprocessed L1 VIIRS data for the Clouds and the Earth's Radiant Energy System (CERES) mission Climate Data Record (CDR). As demonstrated by MODIS and the AVHRR, reprocessing of the VIIRS data record will be essential for the production of climate quality data records that can further research in Earth System Science.

4. Next Steps for VIIRS Land and Cryosphere Products

[39] The VIIRS instrument has a critical role to play in long-term coarse resolution observations of the land surface. After more than a year of on-orbit operations, the land group of the NASA S-NPP Science Team has determined that the VIIRS is an instrument well suited for continuing and further developing the land science currently undertaken using MODIS and in some aspects provides an improvement over the MODIS instrument capability. For example, the VIIRS instrument design constrains pixel growth across the scan and provides complete daily global coverage, which has proven to be an advantage for land and cryosphere products. Similarly, the higher-resolution image bands and day-night band offer enhanced capabilities beyond MODIS [Miller *et al.*, 2012]. However, it is our conclusion that the full potential of VIIRS for global change science and applications will not be exploited through the operational IDPS system as currently configured.

[40] The JPSS program has been designed to meet the needs of the NOAA operational user community (e.g., National Weather Service, National Centers for Environmental Prediction, and Air Force Weather Agency) with product specifications to meet those needs, with no requirement for developing science products or developing a consistent long-term data record needed for global change science. Improvements are slowly being made to the IDPS and EDRs as problems are encountered or proposed improvements made by the VIIRS Algorithm and science teams are accepted, and this will continue until the EDR specifications are met. However, this means that there is no archive of consistently processed data products and there is no reprocessing planned using the IDPS system. In addition, some of the improvements suggested by the Land Science Team will not be accepted; although they would result in better products, as they are incompatible with the configuration of the IDPS processing chain and the current EDR algorithms. A more rapid and nimble system for integration and testing of improvements to VIIRS land and cryosphere products is needed, preferably following the approach developed for MODIS which enables thorough testing of algorithm changes and dependencies on global time series and golden tiles before moving them into production. As with MODIS, the VIIRS data record can now be improved based on the ongoing efforts to better understand the instrument calibration and product accuracy assessment, and in this context periodic reprocessing of the entire data record from VIIRS is essential.

[41] There are a number of land standard products from MODIS which are not currently generated by the IDPS or planned for IDPS production (i.e., Leaf Area Index/Fraction of Photosynthetically Active Radiation(LAI/FPAR), Net Primary Productivity, Vegetation Dynamics (phenology), Vegetation Continuous Fields, and Burned Area). If NASA MODIS product continuity is to be maintained, these products will need to be generated. At the same time both earth system science and remote sensing methods are advancing, and additional global products could be considered, e.g., Evapotranspiration, Forest Cover Change, and Crop Type. Similarly, although there has been considerable investment in regional ground station, Direct Read-Out capability from VIIRS, there is a strong interest from the science and applications communities to obtain global VIIRS data in near-real time with the functionality similar to that of the NASA Land Atmosphere Near-real-time Capability for EOS (LANCE) system [Murphy et al., 2012].

[42] Based on the EDR evaluation experience to-date summarized above, it is strongly recommended that a suite of VIIRS Earth Science Data Records for land science be developed, from the start of the S-NPP VIIRS observations, that will at least provide continuity with the MODIS products. The lesson learned from MODIS is that the data records should be under the stewardship of a group of scientists, responsible for quality and accuracy assessment (QA and validation), product maintenance and documentation, guidance on data reprocessing, and outreach to the science and applications community. Once these products have been promoted to “provisional status,” product validation should be initiated to take the products to at least Committee on Earth Observation Satellites (CEOS) Validation Stage 2 [Morisette et al., 2002]. There will also be some benefit from connecting these global-scale validation activities to the international Land Product Validation (LPV) subgroup of the CEOS

Working Group on Calibration and Validation, as is currently the case with MODIS.

[43] To achieve the stated goal of MODIS data continuity and the establishment of long-term data records through VIIRS, it is important to start now to use S-NPP to establish a pathway to science use of VIIRS data in the JPSS era [Justice et al., 2011]. One year after launch, initial instrument and operational product evaluations are now ending, and the next step is to build on the success of the MODIS Adaptive Processing System and the Land PEATE data processing and generate and distribute high-quality VIIRS land and cryosphere products from the beginning of the VIIRS data record and with the capability of subsequent reprocessing to meet the needs of the land science and applications communities.

References

Barrie, J. D., P. D. Fuqua, M. J. Meshishnek, M. R. Ciofalo, C. T. Chu, J. A. Chaney, R. M. Moision, and L. Graziani (2012), Root cause determination of on-orbit degradation of the VIIRS rotating telescope assembly, *Proc. SPIE 8510, Earth Observing Systems XVII*, 85101B-85101B, doi:10.1117/12.933276.

Bellward, A. S., J. E. Estes, and K. D. Kline (1999), The IGBP-DIS global 1-km land-cover data set DISCover: A project overview, *Photogramm. Eng. Remote Sens.*, 65(9), 1013–1020.

Cescatti, A., et al. (2012), Intercomparison of MODIS albedo retrievals and in situ measurements across the global FLUXNET network, *Remote Sens. Environ.*, 121, 323–334, doi:10.1016/j.rse.2012.02.019.

Csiszar, I., W. Schroeder, L. Giglio, and C. Justice (2012), VIIRS ARP Release, Beta Data Quality (Read-me for Data Users): http://www.class.ncdc.noaa.gov/notification/pdfs/VIIRS_Active%20Fire%20ARP_Release_Readme_final.pdf—Last Updated: 10/22/2012.

Friedl, M. A., et al. (2002), Global land cover mapping from MODIS: Algorithms and early results, *Remote Sens. Environ.*, 83(1–2), 287–302.

Friedl, M. A., D. Sulla-Menashe, B. Tan, A. Schneider, N. Ramankutty, A. Sibley, and X. Huang (2010), MODIS Collection 5 global land cover: Algorithm refinements and characterization of new datasets, *Remote Sens. Environ.*, 114(1), 165–182, doi:10.1016/j.rse.2009.08.016.

He, T., S. Liang, D. Wang, H. Wu, Y. Yu, and J. Wang (2012), Estimation of surface albedo and directional reflectance from Moderate Resolution Imaging Spectroradiometer (MODIS) observations, *Remote Sens. Environ.*, 119, 286–300.

Hook, S. J., R. G. Vaughan, H. Tonooka, and S. G. Schladow (2007), Absolute radiometric in-flight validation of mid infrared and thermal infrared data from ASTER and MODIS on the terra spacecraft using the Lake Tahoe, CA/NV, USA, automated validation site, *IEEE Trans. Geosci. Remote Sens.*, 45(6), 1798–1807.

Huete, A., C. Justice, and W. Leeuwen (1999), MODIS Vegetation Index (MOD 13) Algorithm Theoretical Basis Document Version 3.0. Technical Report (Version 3, 1999, http://modis.gsfc.nasa.gov/data/atbd/atbd_mod13.pdf)*Rep.*, NASA EOS-MODIS.

Hulley, G. C., and S. J. Hook (2009), Intercomparison of versions 4, 4.1 and 5 of the MODIS land surface temperature and emissivity products and validation with laboratory measurements of sand samples from the Namib Desert, Namibia, *Remote Sens. Environ.*, 113, 1313–1318.

Hulley, G. C., and S. J. Hook (2012), A radiance-based method for estimating uncertainties in the Atmospheric Infrared Sounder (AIRS) land surface temperature product, *J. Geophys. Res.*, 117(D20), D20117, doi:10.1029/2012JD018102.

Hulley, G. C., S. J. Hook, and A. M. Baldridge (2010), Generating consistent Land Surface Temperature and Emissivity (LST&E) products between ASTER and MODIS data for earth science research, *IEEE Trans. Geosci. Remote Sens.*, 49(9), 1,304–1,315, doi:10.1109/TGRS.2010.2063034.

Justice, C. O., L. Giglio, S. Korontzi, J. Owens, J. T. Morisette, D. Roy, J. Desclolettes, S. Alleaume, F. Petitcolin, and Y. Kaufman (2002), The MODIS fire products, *Remote Sens. Environ.*, 83(1–2), 244–262.

Justice, C. O., E. Vermote, J. L. Privette, and A. Sei (2011), The evolution of U.S. moderate resolution optical land remote sensing from AVHRR to VIIRS, in *Land Remote Sensing and Global Environmental Change: NASA’s Earth Observing System and the Science of ASTER and MODIS*, edited by B. Ramachandran, C. O. Justice, and M. J. Abrams, pp. 873, Springer Verlag, London, UK.

Liang, S. (2003), A direct algorithm for estimating land surface broadband albedos from MODIS Imagery, *IEEE Trans. Geosci. Remote Sens.*, 41, 136–145.

Lucht, W., C. B. Schaaf, and A. H. Strahler (2000), An algorithm for the retrieval of albedo from space using semi-empirical BRDF models, *IEEE Trans. Geosci. Remote Sens.*, 38, 977–998, doi:10.1109/36.841980.

Masuoka, E. J., R. E. Wolfe, S. Sinno, Y. Gang, and M. Teague (2007), A disk-based system for producing and distributing science products from MODIS, *Proceedings of the Geoscience and Remote Sensing Symposium (IGARSS'07)*, Barcelona, Spain, 3043–3046, doi:10.1109/IGARSS.2007.4423486.

Masuoka, E., D. Roy, R. Wolfe, J. Morisette, S. Sinno, M. Teague, N. Saleous, S. Devadiga, C. O. Justice, and J. Nickeson (2011), MODIS land data products: Generation, quality assurance and validation, in *Land Remote Sensing and Global Environmental Change: NASA's Earth Observing System and the Science of ASTER and MODIS*, edited by B. Ramachandran, C. Justice, and M. Abrams, pp. 873, Springer Verlag, London, UK.

Miller, S. D., S. P. Mills, C. D. Elvidge, D. T. Lindsey, T. F. Lee, and J. D. Hawkins (2012), Suomi satellite brings to light a unique frontier of nighttime environmental sensing capabilities, *PNAS*, 109(39), 15,706–15,711, doi:10.1073/pnas.1207034109.

Morisette, J. T., J. L. Privette, and C. O. Justice (2002), A framework for the validation of MODIS land products, *Remote Sens. Environ.*, 83(1–2), 77–96, doi:10.1016/S0034-4257(02)00088-3.

Murphy, K., C. Justice, D. Lowe, M. Maiden, and D. Davies (2012), LANCE user working group meeting, in *The Earth Observer*, edited, pp. 19–21, NASA GSFC.

Quinlan, J. R. (1996), Bagging, boosting, and c4.5, paper presented at Thirteenth National Conference on Artificial Intelligence, AAAI Press and the MIT Press.

Román, M. O., et al. (2009), The MODIS (Collection V005) BRDF/albedo product: Assessment of spatial representativeness over forested landscapes, *Remote Sens. Environ.*, 113, 2476–2498, doi:10.1016/j.rse.2009.07.009.

Román, M. O., C. Justice, I. Csiszar, J. R. Key, S. Devadiga, C. Davidson, R. Wolfe, and J. Privette (2011), Pre-launch evaluation of the NPP VIIRS land and cryosphere EDRs to meet NASA's science requirements, *Proceedings of the Geoscience and Remote Sensing Symposium (IGARSS'11)*, Vancouver, BC, 154–157, doi:10.1109/IGARSS.2011.6048921.

Román, M. O., I. Csiszar, C. Justice, J. Key, J. Privette, S. Devadiga, C. Davidson, R. E. Wolfe, and E. J. Masuoka (2012), Status of the Suomi NPP visible/infrared imager radiometer suite's (VIIRS) land environmental data records (EDRs) after early evaluation of on-orbit performance, paper presented at Geoscience and Remote Sensing Symposium (IGARSS), 2012 IEEE International, 22–27 July 2012.

Salomonson, V. V., and I. Appel (2004), Estimating the fractional snow cover using the normalized difference snow index, *Remote Sens. Environ.*, 89(3), 351–360.

Schaaf, C. B., et al. (2002), First operational BRDF, albedo and nadir reflectance products from MODIS, *Remote Sens. Environ.*, 83(1–2), 135–148, doi:10.1016/S0034-4257(02)00091-3.

Schaaf, C. B., J. Liu, F. Gao, and A. H. Strahler (2011), MODIS albedo and reflectance anisotropy products from Aqua and Terra, in *Land Remote Sensing and Global Environmental Change: NASA's Earth Observing System and the Science of ASTER and MODIS*, edited by B. Ramachandran, C. Justice, and M. Abrams, pp. 873, Springer-Verlag, London, UK.

Schaepman-Strub, G., M. E. Schaepman, T. H. Painter, S. Dangel, and J. V. Martonchik (2006), Reflectance quantities in optical remote sensing—definitions and case studies, *Remote Sens. Environ.*, 103(1), 27–42, doi:10.1016/j.rse.2006.03.002.

Tucker, C. J. (1979), Red and photographic infrared linear combinations for monitoring vegetation, *Remote Sens. Environ.*, 8(2), 127–150, doi:10.1016/0034-4257(79)90013-0.

Vermote, E. F., N. Z. El Saleous, and C. O. Justice (2002), Atmospheric correction of MODIS data in the visible to middle infrared: First results, *Remote Sens. Environ.*, 83(1–2), 97–111.

Wan, Z. M., and Z. L. Li (1997), A physics-based algorithm for retrieving land-surface emissivity and temperature from EO-8/MODIS data, *IEEE Trans. Geosci. Remote Sens.*, 35(4), 980–996.

Wan, Z. M., and Z. L. Li (2008), Radiance-based validation of the V5 MODIS land-surface temperature product, *Int. J. Remote Sens.*, 29(17–18), 5373–5395.

Wang, Y., A. Lyapustin, J. L. Privette, J. Morisette, and B. N. Holben (2009), Atmospheric correction at AERONET locations: A new science and validation data set, *IEEE Trans. Geosci. Remote Sens.*, 47(1), 2450–2466.

Wang, Z., C. B. Schaaf, A. H. Strahler, J. Wang, C. E. Woodcock, M. J. Chopping, M. O. Román, A. V. Rocha, and Y. Shuai (2012), Evaluation of Moderate-Resolution Imaging Spectroradiometer (MODIS) snow albedo product (MCD43A) over tundra, *Remote Sens. Environ.*, 117, 264–280, doi:10.1016/j.rse.2011.10.002.

Wanner, W., X. Li, and A. H. Strahler (1995), On the derivation of kernels for kernel-driven models of bidirectional reflectance, *J. Geophys. Res.*, 100(D10), 21,077–21,089, doi:10.1029/95JD02371.

Wolfe, R., S. Devadiga, G. Ye, E. Masuoka, and R. J. Schweiss (2010), Evaluation of the VIIRS land algorithms at the Land PEATE, *IEEE Geoscience and Remote Sensing Symposium (IGARSS'10)* Honolulu, HI (204-307), doi:10.1109/IGARSS.2010.5652831.